

## Article

# Biosorption of Hexavalent Chromium by *Bacillus megaterium* and *Rhodotorula* sp. Inactivated Biomass

Mihaela Roșca<sup>1,2,\*</sup> , Bruna Silva<sup>3</sup>, Teresa Tavares<sup>3</sup>  and Maria Gavrilescu<sup>1,4,\*</sup> 

- <sup>1</sup> Department of Environmental Engineering and Management, “Cristofor Simionescu” Faculty of Chemical Engineering and Environmental Protection, “Gheorghe Asachi” Technical University of Iasi, 73 Prof. D. Mangeron Blvd., 700050 Iasi, Romania
- <sup>2</sup> Department of Horticultural Technologies, Faculty of Horticulture, “Ion Ionescu de la Brad” Iasi University of Life Sciences, 3 Mihail Sadoveanu Alley, 700490 Iasi, Romania
- <sup>3</sup> Centre of Biological Engineering, University of Minho, Campus de Gualtar, 4710-057 Braga, Portugal
- <sup>4</sup> Academy of Romanian Scientists, 3 Ilfov Street, 050044 Bucharest, Romania
- \* Correspondence: mihaelarosca@uaiasi.ro (M.R.); mgav@tuiasi.ro (M.G.)

**Abstract:** Due to the adverse effects of hexavalent chromium ( $\text{Cr}^{6+}$ ) on human health and the quality of the environment, the scientific community has invested a lot of effort to solve this pollution problem. Thus, implementing sustainable alternatives for  $\text{Cr}^{6+}$  elimination by exploiting the capacity of microbial biomass to retain heavy metals by biosorption is considered an economic and eco-friendly solution, compared to the conventional physico-chemical processes. However, the ability of microorganisms to remove  $\text{Cr}^{6+}$  from liquid effluents can strongly be affected by biotic and abiotic factors. With these issues in mind, the main purpose of this paper was to investigate  $\text{Cr}^{6+}$  biosorption on *Bacillus megaterium* and *Rhodotorula* sp. biomass inactivated by thermal treatments, exploring the effects of some factors such as: pH, biosorbent dose, initial concentration of the metal in solution, temperature and contact time between the biosorbent and the metal ions on process effectiveness. The results showed that  $\text{Cr}^{6+}$  removal by biosorption on the selected microorganisms was strongly influenced by the pH of the solution which contains chromium, the reduction being the principal mechanism involved in hexavalent chromium biosorption. Equilibrium and kinetic studies were also performed, together with SEM-EDX and FTIR spectra, to explain the mechanisms of the biosorption process on the selected biomasses. Maximum uptake capacities of 34.80 mg/g biosorbent and 47.70 mg/g biosorbent were achieved by *Bacillus megaterium* and *Rhodotorula* sp., respectively, at pH 1, biosorbent dosage of 8 g/L, 25 °C, after a contact time of 48 h and an initial  $\text{Cr}^{6+}$  concentration in solution of 402.52 mg/L. The experimental results showed that  $\text{Cr}^{6+}$  biosorption by selected microorganisms followed the Elovich model, the values of the correlation coefficients being 0.9868 and 0.9887, respectively. The Freundlich isotherm model best describes the  $\text{Cr}^{6+}$  biosorption by *Bacillus megaterium* and *Rhodotorula* sp., indicating that a multilayer biosorption mainly controls the process and is conducted on heterogeneous surfaces with uniformly distributed energy.

**Keywords:** abiotic factors; *Bacillus megaterium*; biosorption; hexavalent chromium; *Rhodotorula* sp.



**Citation:** Roșca, M.; Silva, B.; Tavares, T.; Gavrilescu, M. Biosorption of Hexavalent Chromium by *Bacillus megaterium* and *Rhodotorula* sp. Inactivated Biomass. *Processes* **2023**, *11*, 179. <https://doi.org/10.3390/pr11010179>

Academic Editor: José A. Peres

Received: 12 December 2022

Revised: 29 December 2022

Accepted: 31 December 2022

Published: 6 January 2023



**Copyright:** © 2023 by the authors. Licensee MDPI, Basel, Switzerland. This article is an open access article distributed under the terms and conditions of the Creative Commons Attribution (CC BY) license (<https://creativecommons.org/licenses/by/4.0/>).

## 1. Introduction

The presence of heavy metals in water bodies in high concentrations, as a result of anthropogenic activities, is a serious problem for the environment and human health. At the European level, according to the European Pollutant Release and Transfer Register (E-PRTR) database, the industrial activities from the energy sector, mining industry, metal processing and production industry, urban wastewater treatment, pulp, paper and cardboard manufacturing and chemical industry continue to release high quantities of heavy metals into water. Some figures show that these industrial activities discharged 1895 tons of zinc, 911 tons of copper, 834 tons of chromium, 260 tons of nickel, 86.4 tons of lead, 70.1 tons of arsenic, 13.9 tons of cadmium and 3.78 tons of mercury into Europe's rivers in

2017 [1]. These metals are then accumulated in soil and sediments and enter in the food chain, causing harmful effects on all forms of life [2,3].

Among the most hazardous heavy metals discharged into surface water from various activities is chromium [4,5]. As a chemical element, it belongs to the transition metal category and occurs naturally in the earth's crust in the ore chromite, in the oxidation state 3+ ( $\text{Cr}^{3+}$ ). This ore is used to make monochromate, dichromate, chromic acid and chromium-based pigments, as well as the metal itself [6,7]. The oxidation states of this metal are from  $-2$  to  $+6$ , but it is stable in the environment only as  $\text{Cr}^0$  (elemental form),  $\text{Cr}^{3+}$  and  $\text{Cr}^{6+}$ , forms that show different toxicity and mobility behaviors in the environment [8]. The hexavalent form is the most hazardous, being considered 1000 times more toxic than the trivalent form [5,9].

Due to their properties, chromium compounds continue to be used in many industrial processes such as industrial welding, dyes and pigments manufacturing, electroplating processes, leather tanning and wood preservation, etc., but making chromium a major environmental pollutant [7,8,10], since the unsustainable use and waste management determine its presence in industrial effluents in different concentrations. In some electroplating effluents, for instance,  $\text{Cr}^{6+}$  concentration ranged from 6 mg/L to 887 mg/L [11–14], while in the leather processing liquid effluents, the average  $\text{Cr}^{6+}$  concentration was found of about 821 mg/L [15]. At an extreme level, in textile dyeing effluents,  $\text{Cr}^{6+}$  can reach concentrations of 1300–2500 mg/L [16].

Thus, the removal followed by the possible recovery of heavy metals from industrial wastewater are among the extremely important measures that can be applied to reduce heavy metal pollution of water and minimize their risks to human health [17–19]. The application of biotechnology in the control and reduction of environmental pollution with metals has become a sustainable alternative to conventional processes. Among of the most applied biological processes for the remediation of polluted environments are biosorption and bioaccumulation by natural biological materials (e.g., plants, microorganisms—for biosorption/bioaccumulation, agriculture waste—for biosorption) [18,20–24].

Microorganisms can remove the metal ions both in viable or inactivated, dead forms by several mechanisms [23]. Research so far has shown that the use of viable microorganisms for the retention of chromium from wastewater is actually at a disadvantage because living cells are affected by the toxicity of the heavy metal, which through bioaccumulation can reach concentrations at the level of cells that can cause cell death [5,20,24,25]. Therefore, the use of inactivated microbial cells has the advantage that the effectiveness of the microbial biomass used as a biosorbent is not reduced over time as a result of the toxicity of the retained metal [24,25]. Biosorption was studied in a series of papers, the vast majority used vegetable waste of agricultural origin as biosorbents, and less microbial biomass. [25–28]. *Saccharomyces cerevisiae* has been used, for example, for biosorption of lead [23], cadmium, chromium [29]. *Trichoderma viride* [30], *Bacillus cereus* M<sup>1</sup><sub>16</sub> [31], *Rhodotorula* sp. Y11 [32], etc., and it has been shown to have a high affinity for  $\text{Cd}^{2+}$  removal from aqueous solutions and *Bacillus subtilis* MNU16 has a high tolerance and ability in reducing  $\text{Cr}^{6+}$  to  $\text{Cr}^{3+}$  [33]. *Bacillus megaterium* and *Rhodotorula* sp. inactivated biomass have been proved to be able to remove  $\text{Cd}^{2+}$  from aqueous solutions, possessing a biosorption capacity of 15.1 mg/g and 14.2 mg/g, respectively [34].

Thus, this research aimed to investigate the effectiveness *B. megaterium* and *Rhodotorula* sp. inactivated biomass for  $\text{Cr}^{6+}$  biosorption under the influence of pH, biosorbent dose, initial concentration of the metal in solution, temperature at which the process takes place and the contact time between biosorbent and chromium ions. In order to understand the mechanism by which the selected biosorbents removed  $\text{Cr}^{6+}$ , the experimental data were evaluated by using equilibrium sorption isotherms and kinetic models. Furthermore, the biosorbents were characterized before and after biosorption by Fourier-transform infrared spectroscopy (FTIR) and scanning electron microscopy coupled with energy dispersive X-ray spectroscopy (SEM-EDS). So, the information provided by this study will contribute

to the comprehension of the  $\text{Cr}^{6+}$  biosorption by the microorganism with the possibility of further exploitation of this at pilot and even industrial scale.

## 2. Materials and Methods

### 2.1. Biosorbents Preparation

The protocol used for the isolation and identification of *Bacillus megaterium* and *Rhodotorula* sp., as well as the preparation of inactive biomass for chromium biosorption was previously published by Roşca et al. [34] in 2018. The crushed dried inactive biomass of *Bacillus megaterium* and *Rhodotorula* sp. was stored in a desiccator until further use.

### 2.2. Biosorption Studies

$\text{Cr}^{6+}$  biosorption by *Bacillus megaterium* and *Rhodotorula* sp. were carried out using analytical grade substances. In 500 mL distilled water, 1.4144 g  $\text{K}_2\text{Cr}_2\text{O}_7$  (Riedel-de Haën, Seelze, Germany) was dissolved to prepare the stock solution with the concentration of 1000 mg/L. Subsequently, by the dilution of the stock solution with distilled water, the working solutions were prepared. For each set of experiments the initial pH of solutions was adjusted using 0.1 M  $\text{HNO}_3$  or 0.1 M  $\text{NaOH}$  and measured with ProLab 2000 multiparameter equipped with a glass electrode.

The biosorption of  $\text{Cr}^{6+}$  was studied in a batch system, in 200 mL Erlenmeyer flasks with 50 mL  $\text{Cr}^{6+}$  solution. For the kinetic studies 100 mL  $\text{Cr}^{6+}$  solution were used. The values of the influencing factors for each set of performed experiments are shown in Table 1. All experiments were carried out in duplicate, in IKA 4000 IC incubator at 150 rpm.

**Table 1.** Values of influencing factors used in experimental studies for  $\text{Cr}^{6+}$  biosorption.

Experiments	Factors Values				
	pH	Biosorbent Dose (g/L)	Contact Time (Minutes)	Initial Concentration (mg/L)	Temperature (°C)
1—Effect of initial pH	1–5	5	2880	51.03	25
2—Effect of biosorbent dose	1	1–10	2880	51.03	25
3—Effect of contact time	1	8	10–4320	96.29	25
4—Effect of initial concentration	1	8	2880	25.29–402.52	25
5—Effect of temperature	1	8	2880	201.87	25–40

The values of the influence factors at which the efficiency of the biosorption process was maximum were considered as the optimal values for  $\text{Cr}^{6+}$  biosorption. During the experiments, the optimum value of an experimentally established factor was used to study the influence of other factors. The separation of the liquid phase from the solid phase was achieved by centrifugation at 7000 rpm for 10 min.

### 2.3. Determination of Metal Concentration in Solution

The concentration of hexavalent chromium ions in solution was determined by UV–VIS spectrometry according to METHOD 7196 [35] (Table 2) with a PG Instruments T60 UV–VIS spectrophotometer and 1 cm thick quartz cuvettes.

**Table 2.** Determination of  $\text{Cr}^{6+}$  concentration in solution.

Parameter	Value
Optimum pH	2
Color Reagent	Diphenyl carbazide in acetone, 5 g/L
Buffer	$\text{H}_2\text{SO}_4$ , 10%
Wavelength ( $\lambda_{\text{max}}$ , nm)	540
Reference sample	Blank
Linear range, (mg/L)	0.1–1
Equation	$y = 0.7588x + 0.0127$
Regression coefficient	0.9997

Measurement of total chromium concentration in solution was performed by inductively coupled plasma spectrometer (Optima 8000 ICP-OES model, PerkinElmer, Inc., Waltham, MA, USA) at 283.56 nm wavelength. Prior to analysis, the samples were acidified with nitric acid (69%) (Fisher Scientific, Loughborough, Leicestershire, UK) to an acid concentration of approximately 2% and filtered with 0.2  $\mu\text{m}$  nylon filters. The samples were stored at 4 °C until the concentration of metal ions in solution was measured.

#### 2.4. Quantification of Biosorption Performances

The performance of  $\text{Cr}^{6+}$  biosorption by *B. megaterium* and *Rhodotorula* sp. inactivated biomass were assessed using the following quantitative parameters:

- biosorption capacity ( $q$ , mg/g) which is defined as the amount of metal taken up by the biosorbent per unit mass (or volume) of biosorbent under established experimental conditions, being calculated with Equation (1).

$$q = \frac{(C_0 - C) \cdot V}{m} \quad (1)$$

- removal efficiency ( $R$ , %) is the fraction of metal removed expressed in percent and can be calculated using Equation (2):

$$R\% = \frac{(C_0 - C)}{C_0} \cdot 100 \quad (2)$$

where:  $C_0$ ,  $C$ —initial and residual concentration of metal ion in solution, respectively (mg/L);  $m$ —biosorbent mass (g);  $V$ —volume of aqueous solution that was used in biosorption studies (L).

#### 2.5. Biosorption Kinetics

Four of the most widely used kinetic models were applied to describe the mechanism of  $\text{Cr}^{6+}$  biosorption: pseudo I-order model, pseudo II-order model, Elovich model and intraparticle diffusion model. Non-linear regression was used to choose the most appropriate kinetic model for the experimental data, and the corresponding correlation coefficients were calculated in Origin Pro 8 software. The choice of kinetic model best describing the experimental data was made by comparing the correlation coefficients ( $R^2$ ) of each model and the adequate model was considered to be the one with  $R^2$  closest to unity. The kinetic models were chosen taking into account the information that each model provides and their usefulness in identifying the possible mechanisms involved in  $\text{Cr}^{6+}$  biosorption.

The pseudo I kinetic model assumes that the rate of metal ion adsorption is proportional to the number of free adsorption centers. Additionally, this model considers that, following the cation interaction with functional groups on the biosorbent surface, a transition complex (generically referred to as an “activated complex”) is initially formed, which then, through stabilization, enables their retention on the biosorbent surface [26,36,37]. The pseudo II order kinetic model hypothesizes that the solute adsorption rate is proportional to the available sites on the adsorbent surface and the interactions between biosorbent and solute are predominantly chemical (ion exchange or complexation) [26,36]. This model describes the kinetics of most biosorption systems, in which the adsorbent material has functional groups with different but close affinities on its surface that interact directly with metal ions in the aqueous solution [36]. The Elovich model predicts the diffusion, activation and deactivation energies of the mass and surface of a system. The model assumes that the solute sorption rate decreases exponentially as the amount of sorbed solute increases [36]. The internal diffusion model asserts that the internal diffusion of the adsorbate is the slowest step, hence it is the step that controls the rate during the adsorption process, and adsorption is instantaneous. Therefore, the biosorption kinetic depend on the pore size of the adsorbent material and the preparation of the biosorbent will significantly influence the process efficiency [38].

## 2.6. Adsorption Isotherms

Nonlinear forms of Freundlich, Langmuir, Redlich-Peterson, Jovanovic, Hill and Dual Mode isotherm models were applied in Origin Pro 8 software for analysis of experimental data. The mathematical models were chosen taking into account the information that each isotherm model provides and their usefulness in describing the  $\text{Cr}^{6+}$  biosorption.

The Langmuir model provides information about the maximum sorption capacity and the behavior of the sorption process at equilibrium, which can be useful for benchmarking the biosorptive performance of a biosorbent versus other adsorbent materials. This model assumes that the biosorption takes place until a complete monolayer is formed on the biosorbent surface. The Freundlich isotherm describes the multilayer adsorption and considers that it takes place on heterogeneous surfaces with uniformly distributed energy. During the adsorption the stronger binding centers are occupied first, then the others until the adsorption energy decreases [39,40]. The Freundlich model is used to estimate the intensity of the biosorption process and based on this model it can be determined if the biosorption is favorable under the given experimental conditions, with the condition  $1 < n < 10$  [41]. The Redlich-Peterson isotherm is a combination of the Langmuir and Freundlich isotherms. This model is described by an empirical equation that incorporates three parameters and considers that the adsorption mechanism is a mixture and the adsorption is not monolayer [41]. The Hill isotherm describes the binding of different metals to homogeneous substrates and supposes that adsorption is a cooperative phenomenon and adsorbates have the ability to bind to an active center on the biosorbent surface, but could influence other binding centers located on the biosorbent surface [41,42]. The Jovanovic model is based on the assumptions of the Langmuir model, but also considers the possibility of mechanical contacts between adsorbent and metal ions [41,43]. The Dual Mode Model was proposed by Vieth and Sladek [44] and combines the Langmuir equation with a partition mechanism [45].

## 2.7. Biosorbent Characterization Methods

Characterization of biosorbents with respect to  $\text{Cr}^{6+}$  biosorption is fundamental for understanding the mechanism of metal removal. Both Fourier-transform infrared spectroscopy (FTIR) and scanning electron microscopy coupled with energy dispersive X-ray spectroscopy (SEM-EDS) were applied for this purpose. These analyses were carried out as indicated by Roşca et al. [34]. Infrared spectrometry of chromium ion-loaded and unloaded inactive biomass was performed with a BOMEN MB 104 spectrometer and the absorption bands in the sample spectra were identified by using the correlation tables available in the literature. The SEM-EDS analyses were conducted with JEOL JSM 7001F instrument (SEM) coupled with the Oxford INCA 250 (EDS) at 5 kV.

## 3. Results and Discussion

### 3.1. Effect of Initial pH on $\text{Cr}^{6+}$ Biosorption

Analyzing the influence of pH on the  $\text{Cr}^{6+}$  biosorption by the inactive biomass of *B. megaterium* and the yeast *Rhodotorula* sp. was carried out considering the initial pH variation in the range 1–5, 5 g/L biosorbent dose, temperature of 25 °C, initial ion concentration in solution of 51.04 mg/L and maximum contact time 48 h. At the end of the experiments both  $\text{Cr}^{6+}$  and total chromium concentrations in solution were determined. The process efficiency and uptake capacity at each pH value, respectively, were calculated, and the results were graphically represented in Figure 1. Under the established experimental conditions, the highest  $\text{Cr}^{6+}$  biosorption efficiency by *B. megaterium* and *Rhodotorula* sp. (80.22% and 94.10%, respectively) was achieved at pH 1. Experimental results revealed that increasing the pH by one unit (to pH = 2) resulted in a  $\text{Cr}^{6+}$  biosorption efficiency for *B. megaterium* and *Rhodotorula* sp. of only 36.34% and 63.27%, respectively. At pH 5 the efficiency of the biosorption by the selected biosorbent decreased to 14.71% and 15.93%, respectively. The maximum uptake capacities under experimental conditions were 8.19 mg/g (*B. megaterium*) and 9.61 mg/g (*Rhodotorula* sp.), respectively. Decreases in  $\text{Cr}^{6+}$  biosorption efficiency as well

as uptake capacity with pH increasing have also been reported in other studies for *Quercus crassipes* bark [46], *Sinorhizobium* sp. [47], *Arthrobacter viscosus* [48] or *Pleurotus ostreatus* [49] used as biosorbents for  $\text{Cr}^{6+}$  removal from aqueous media.

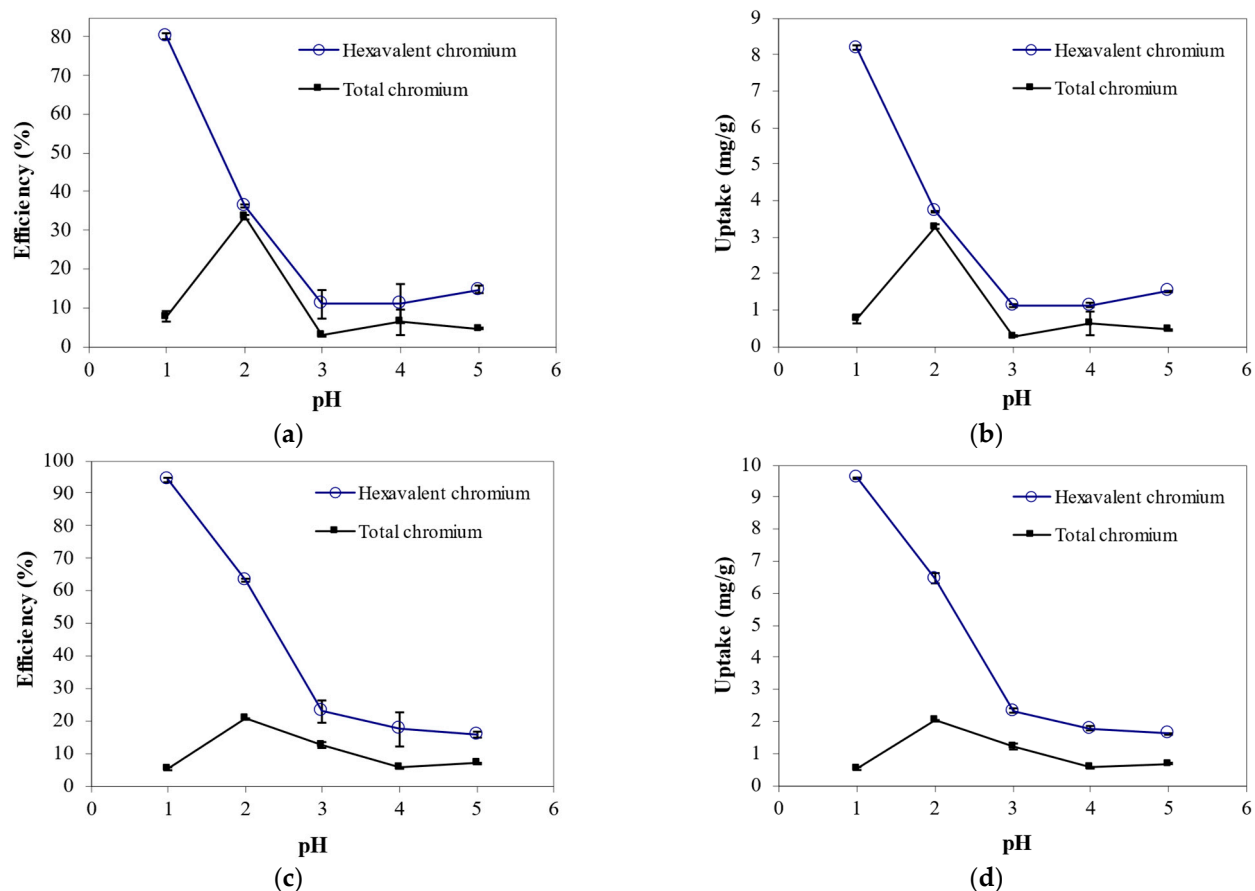


**Figure 1.** Effect of the initial solution pH on (a) process efficiency and (b) chromium uptake by *Bacillus megaterium* inactive biomass and on (c) process efficiency and (d) chromium uptake by *Rhodotorula* sp. inactive biomass (biosorbent dose = 5 g/L, contact time = 48 h, temperature = 25 °C, initial concentration = 51.04 mg/L).

The measurement of total chromium concentration at the end of experiments showed that the efficiency and uptake capacity are considerably low compared to those obtained for hexavalent chromium. The highest values of total chromium biosorption efficiency and uptake capacity were obtained at the initial solution pH of 2. At this value the total chromium biosorption efficiency was 33.46% for *B. megaterium* and *Rhodotorula* sp. removed the total chromium from solution with an efficiency of 20.66%.

Comparing the values of hexavalent chromium concentrations with those of total chromium at the end of the process, it can be stated that the  $\text{Cr}^{6+}$  biosorption is based on the  $\text{Cr}^{6+}$  reduction to the trivalent form. The increase in  $\text{Cr}^{6+}$  removal at lower pH can be attributed to the strong electrostatic attraction between the positively charged ligands found on the biosorbent surface and the negatively charged  $\text{Cr}^{6+}$  oxyanions. Moreover, hydronium ions are involved in the reduction of  $\text{Cr}^{6+}$  to  $\text{Cr}^{3+}$ , whose availability in solution increases with pH decrease. However, as pH increases, the concentration of hydronium ions decreases and the surface charge of the biosorbent becomes negative, impairing the biosorption of negatively charged ion species [46]. The low biosorption efficiency of total chromium can be explained by the fact that at pH below 4, the concentration of hydronium ions in solution is elevated and they load on the biosorbent surface, competing strongly with  $\text{Cr}^{3+}$  for the active sites of the biosorbent. As the pH increases, the concentration of hydronium ions decreases, thus enhancing the binding of  $\text{Cr}^{3+}$  to the biosorbent surface.

### 3.2. Effect of Biomass Dosage on $\text{Cr}^{6+}$ Biosorption

The metal removal efficiency depends significantly on the biosorbent quantity used during the process, with numerous studies reporting that the biosorption efficiency of metal ions increases with increasing the biosorbent dosage. This behavior is a consequence of the higher availability of active centres found on the biosorbent surface when its concentration in solution increases [50]. To determine the effect of biosorbent dosage on the biosorption efficiency of  $\text{Cr}^{6+}$ , experimental studies were performed at 5 different biosorbent doses (1, 3, 5, 8 and 10 g/L) and the results are shown in Figure 2.

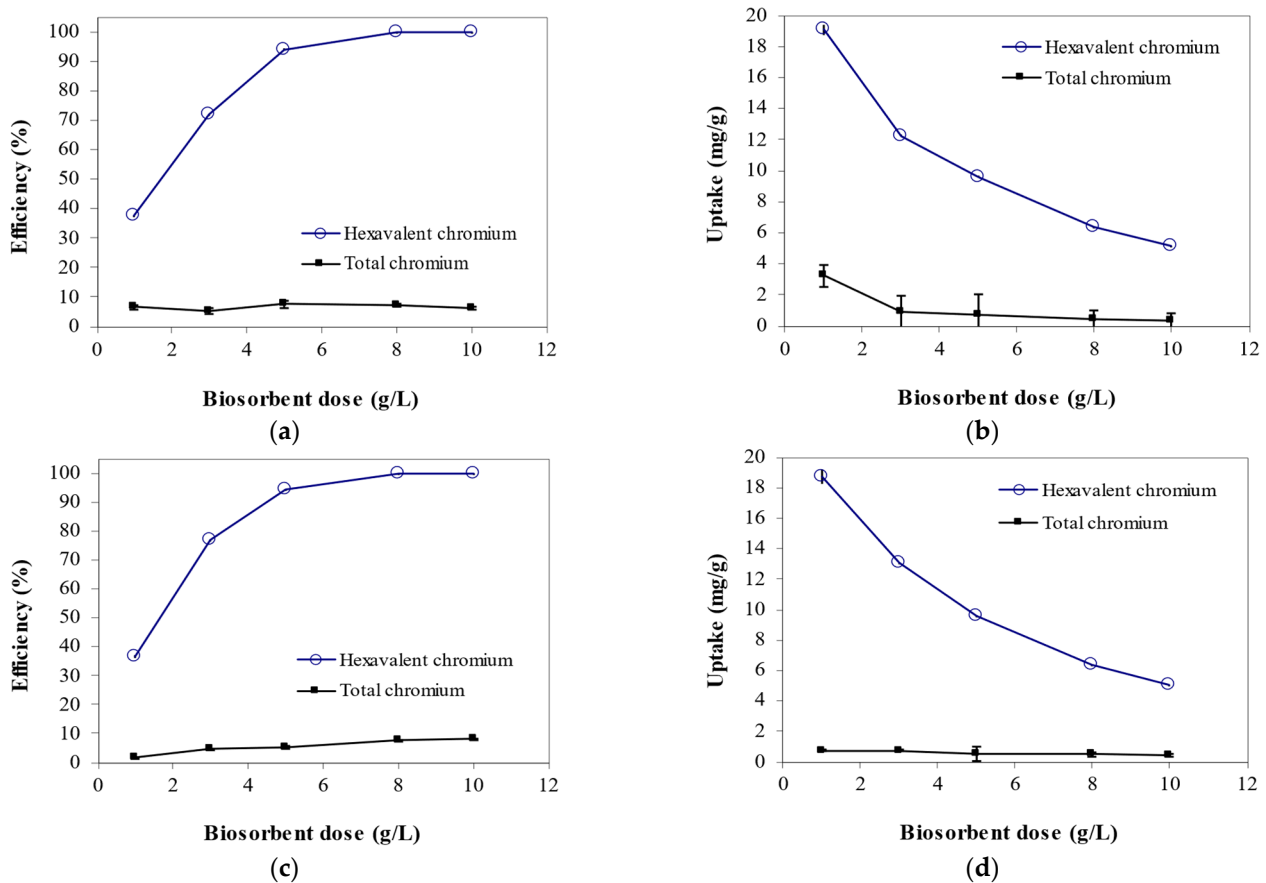


**Figure 2.** Effect of the biosorbent dosage on (a) process efficiency and (b) chromium uptake by *Bacillus megaterium* inactive biomass and on (c) process efficiency and (d) chromium uptake by *Rhodotorula* sp. inactive biomass (pH = 1, contact time = 48 h, temperature = 25 °C, initial concentration = 51.04 mg/L  $\text{Cr}^{6+}$ ).

The results of this study pointed out that the efficiency of the  $\text{Cr}^{6+}$  biosorption increased with increasing of biosorbent dose, the maximum efficiency being 99.98% for *B. megaterium* and 99.79% for *Rhodotorula* sp. at 10 g/L biosorbent dose, pH 1, 48 h contact time, temperature 25 °C and 51.04 mg/L initial concentration of  $\text{Cr}^{6+}$  in solution. At the dose of 1 g/L the process efficiency was 37.35% for *B. megaterium* and 36.72% for *Rhodotorula* sp., values that increase to 94.05% and 94.10% at the 5 g/L, respectively to 99.91% and 99.60% at the 8 g/L. The maximum uptake capacity was recorded at 1 g/L (19.06 mg/g for *B. megaterium* and 18.74 mg/g for *Rhodotorula* sp.) and the minimum at 10 g/L (5.10 mg/g and 5.08 mg/g, respectively). Because the removal efficiencies of  $\text{Cr}^{6+}$  ions are above 99% at a biomass dosage  $\geq 8$  g/L, in this study was considered as optimum value of biomass dosage 8 g/L.

### 3.3. Effect of Contact Time on $\text{Cr}^{6+}$ Biosorption

For the optimization of  $\text{Cr}^{6+}$  biosorption by the inactive biomass of the *B. megaterium* and *Rhodotorula* sp., it was necessary to study the influence of contact time on the removal of

metal ions from the liquid medium. Therefore, in the interval 0–48 h several samples were taken to determine whether the process is a fast one or a slower one. These studies were carried out at an initial concentration of approximately 100 mg/L, pH 1 and biosorbent dose of 8 g/L. The efficiency of chromium biosorption over time was graphically represented in Figure 3. Under the established experimental conditions, after a contact time of 48 h *B. megaterium* removed from aqueous solution 98.76% of the  $\text{Cr}^{6+}$  and *Rhodotorula* sp. 98.99%. Comparing these values with those obtained after only 24 h contact time (91.08% and 98.95%, respectively) it can be stated that *Rhodotorula* sp. removes  $\text{Cr}^{6+}$  faster than *B. megaterium*. The maximum uptake capacity of  $\text{Cr}^{6+}$  at the initial concentration of 101.23 mg/L was 11.89 mg/g (*B. megaterium*) and 12.03 mg/g (*Rhodotorula* sp.), respectively. Total chromium retention is achieved with an efficiency of 7.77% (*B. megaterium*) and 5.94% (*Rhodotorula* sp.) after 48 h of contact, when the maximum efficiency for hexavalent chromium was reached. Similar results were reported by Ojiagu et al. [51] who studied the ability of *Pseudomonas aeruginosa* to remove  $\text{Cr}^{6+}$  from aqueous solutions.

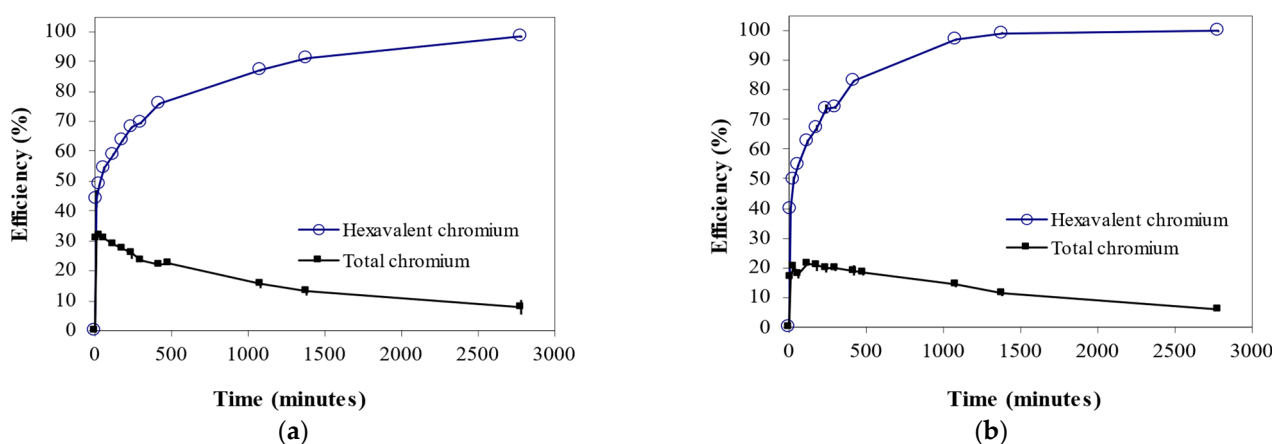


**Figure 3.** Contact time effect on chromium biosorption efficiency by inactive biomass of (a) *B. megaterium* and (b) *Rhodotorula* sp. (pH = 1, biosorbent dose = 8 g/L, temperature = 25 °C, initial concentration = 101.23 mg/L).

### 3.4. Effect of Initial $\text{Cr}^{6+}$ Concentration on Biosorption

The initial concentration of heavy metal ions in solution is another important factor for biosorption, its variation allowing the determination of the maximum amount of metal ion that a biosorbent unit can remove. In the  $\text{Cr}^{6+}$  concentration range 25.29–402.52 mg/L it was found that the uptake capacities of the both biosorbents, increased with concentration increasing and process efficiency decreased. The results of this study showed that at the initial concentration of 402.52 mg/L, *B. megaterium* and *Rhodotorula* sp. removed the  $\text{Cr}^{6+}$  from solution with an efficiency of 69.29% and 94.95%, respectively. At this concentration, *B. megaterium* has an uptake capacity of 34.81 mg/g and *Rhodotorula* sp. 47.70 mg/g. The uptake capacities of the biosorbents as a function of initial  $\text{Cr}^{6+}$  concentrations in solution have been plotted in Figures 4 and 5 and was found that, in the concentration range analyzed, the selected biosorbents did not reach their maximum uptake capacities. According to these results it can be stated that *B. megaterium* and *Rhodotorula* sp. can remove a higher amount of  $\text{Cr}^{6+}$  per gram of biosorbent. From the comparison of the obtained results, it can be seen that *Rhodotorula* sp. removed  $\text{Cr}^{6+}$  from the solution with a higher capacity than inactive bacterial biomass. Srinath et al. [52] reported similar values of uptake capacity for  $\text{Cr}^{6+}$  by inactive biomass of *Bacillus* species (e.g., 39.9 mg/g for *Bacillus circulans* and 30.7 mg/g *Bacillus megaterium*).



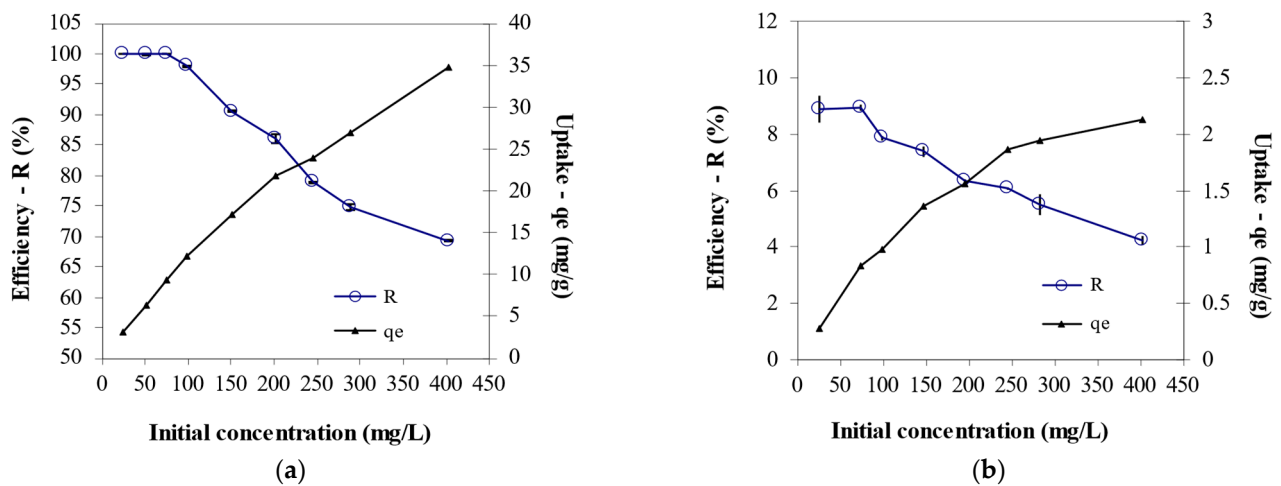


**Figure 4.** Effect of initial metal concentration on biosorption efficiency and metal uptake capacity of (a) Cr<sup>6+</sup> and (b) total chromium by *B. megaterium* inactive biomass (pH = 1, contact time = 48 ore, biosorbent dosage = 8 g/L, temperature = 25 °C).

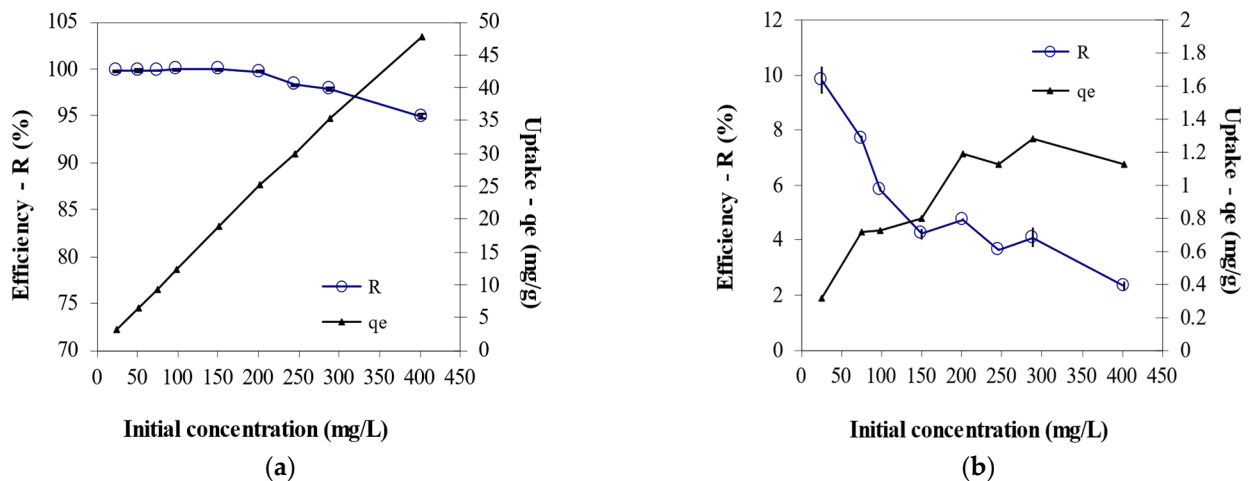


**Figure 5.** Effect of initial metal concentration on biosorption efficiency and metal uptake capacity of (a) Cr<sup>6+</sup> and (b) total chromium by *Rhodotorula* sp. inactive biomass (pH = 1, contact time = 48 ore, biosorbent dosage = 8 g/L, temperature = 25 °C).

Under the established experimental conditions, the uptake capacity of total chromium was determined to be maximum 2.13 mg/g for *B. megaterium* and 1.28 mg/g for *Rhodotorula* sp. at the initial concentrations of 402.52 mg/L.

### 3.5. Effect of Temperature on Cr<sup>6+</sup> Biosorption

Studies on the influence of temperature have been carried out, considering that temperature is one of the parameters that could significantly influence the biosorption of metal ions by the inactive biomass of microorganisms. It has been shown that adsorption processes tend to be exothermic and their performance varies with temperature [53,54]. Biosorption is not a strongly exothermic process compared to other physical adsorption reactions, but temperature variation can influence the performance of the process [30,54]. According to the review article published by Tang et al. [55] the best biosorption performances of Cr<sup>6+</sup> from liquid media by different biosorbents were obtained at temperatures lower than 40 °C. So, the study of the temperature effect on the Cr<sup>6+</sup> biosorption by *B. megaterium* and *Rhodotorula* sp. was carried out in the temperature range 25–40 °C, and the uptake capacities recorded were graphically represented in Figure 6. Experiments showed that the

selected biosorbents have the maximum uptake capacity at 25 °C. At this temperature and an initial Cr<sup>6+</sup> concentration of 201.90 mg/L, the *B. megaterium* inactive biomass removed the Cr<sup>6+</sup> from solution with an efficiency of 83.85% and *Rhodotorula* sp. with an efficiency of 98.72%. With increasing of temperature, the biosorption efficiency decreases to 75.27% and 96.30% at 30 °C, respectively, and then increases with increasing temperature. For total chromium, the best results were achieved at 25 °C by *B. megaterium* and at 30 °C by *Rhodotorula* sp.

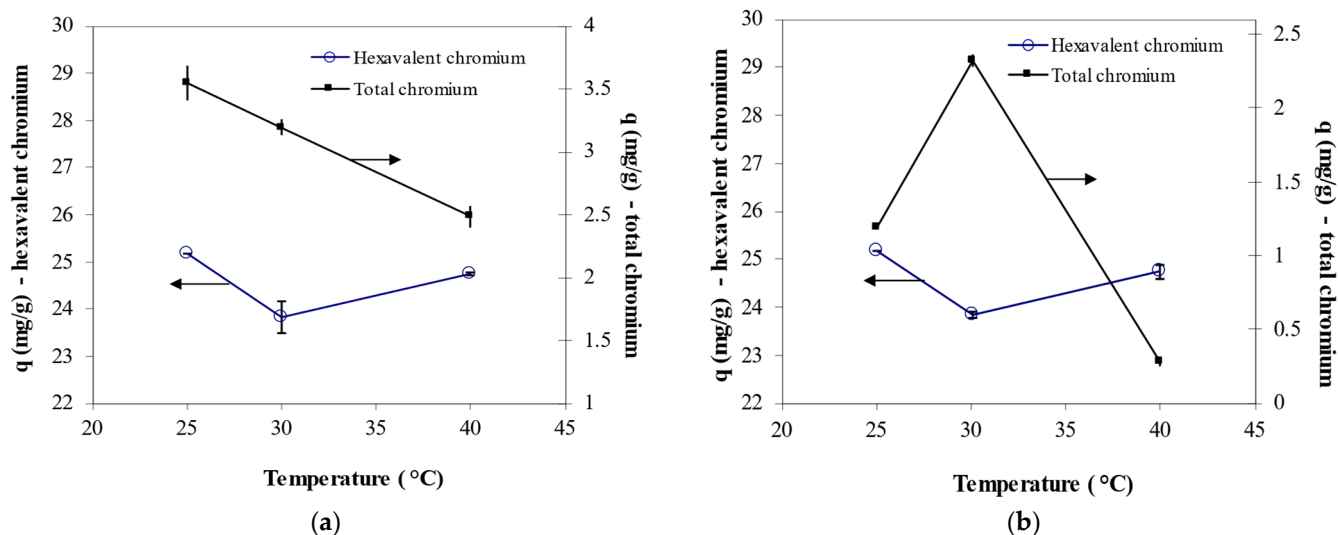


**Figure 6.** Effect of temperature on Cr<sup>6+</sup> and total chromium biosorption efficiency and metal uptake capacity by (a) *B. megaterium* and (b) *Rhodotorula* sp. inactive biomass (pH = 1, biosorbent dose = 8 g/L, contact time = 48 h, initial concentration = 201.90 mg/L).

Dawodu et al. (2020), who studied the influence of temperature variation between 25 and 55 °C on the Cr<sup>6+</sup> biosorption process by *Heinsia crinita* seeds, obtained similar results. They observed a decrease in efficiency with increasing temperature up to 40 °C and then an increase with increasing of temperature.

### 3.6. Sorption Kinetics

The kinetic characterization of heavy metal biosorption processes is one of the most important issues in designing and/or scaling up of the process [56,57]. These studies give insights into the mechanisms involved in metal ion biosorption, mass transfer or chemical interactions [26,56,58]. Characterization of the metal ion biosorption in kinetic terms is necessary since the hydraulic retention time and reactor dimensions are controlled by the contact time between metal ions and biosorbent required to achieve the desired performance. During biosorption, the largest amount of metal is biosorbed in the first minutes to hours because all active sites on the biosorbent surface are free and available for the metal ions biosorption [27]. In this study, four of the most widely used kinetic models were applied to describe the mechanism of chromium biosorption (pseudo I order, pseudo II order, Elovich model and intraparticle diffusion model). Their graphical representations to the kinetic data are shown in Figure 7, and the values of kinetic parameters and the nonlinear correlation coefficients are included in Table 3. By analyzing both the graphical representations and the values of kinetic parameters, it could be determined that the Elovich model is the most suitable to describe the kinetics of the Cr<sup>6+</sup> biosorption by *B. megaterium* and *Rhodotorula* sp. inactive biomass. The values of the correlation coefficients are greater than 0.9868 and initial adsorption rate of 4.091 mg/g·min and 2.684 mg/g·min, respectively (Table 3).

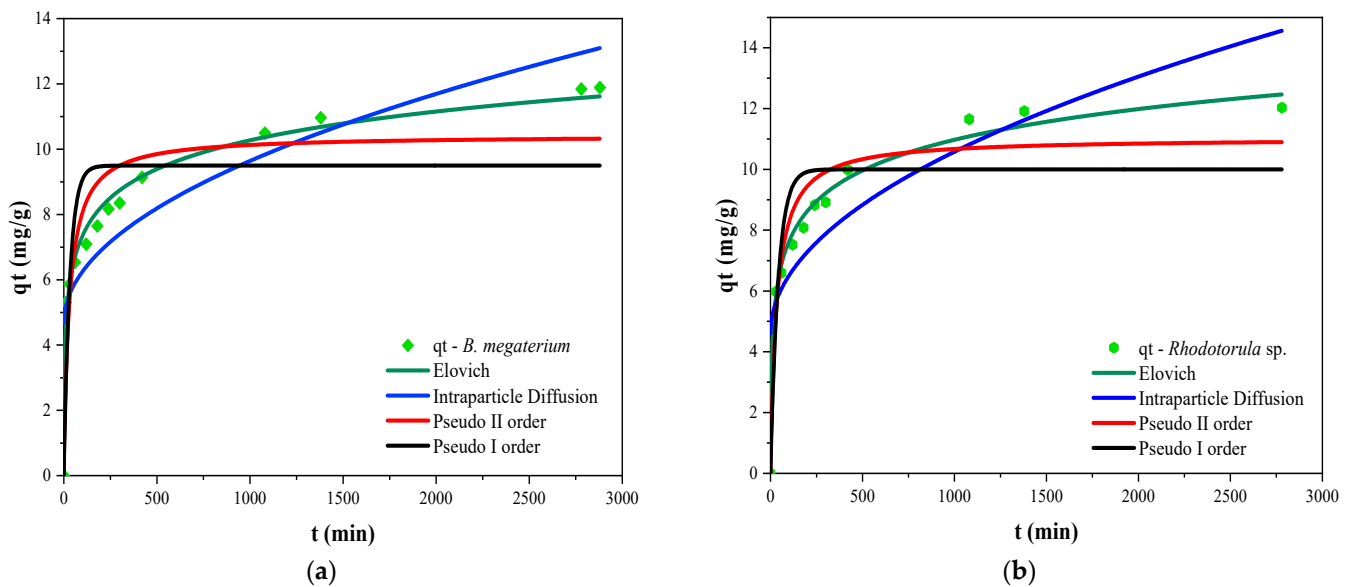


**Figure 7.** Plots of non-linear forms of pseudo I order model, pseudo II order model, Elovich model and intraparticle diffusion model for  $\text{Cr}^{6+}$  biosorption by (a) *Bacillus megaterium* and (b) *Rhodotorula* sp. inactive biomass.

**Table 3.** Values of the kinetic models' parameters for  $\text{Cr}^{6+}$  biosorption by *Bacillus megaterium* and *Rhodotorula* sp. inactive biomass.

Kinetic Model	Parameters	<i>B. megaterium</i>		<i>Rhodotorula</i> sp.	
		Parameter Value	SE	Parameter Value	SE
Pseudo I order	$k_1$	0.031	0.012	0.024	0.008
	$q_e$ (mg/g)	9.496	0.611	10.001	0.635
	$R^2$	0.7169	-	0.7821	-
Pseudo II order	$k_2$	0.003	0.001	0.003	0.001
	$q_e$ (mg/g)	10.427	0.584	11.029	0.587
	$R^2$	0.8451	-	0.8947	-
Elovich	$\alpha$ (mg/g·min)	4.091	1.324	2.684	0.740
	$\beta$ (mg/g·min)	0.786	0.042	0.685	0.036
	$R^2$	0.9868	-	0.9887	-
Intraparticle diffusion	$k_{diff}$ (mg/g)	0.157	0.027	0.189	0.036
	$C_e$ (mg/L)	4.684	0.725	4.614	0.855
	$R^2$	0.7559	-	0.7282	-
$q$ experimental		11.888	0.004	12.031	0.016

SE = Standard Error;  $k_1$  = rate constant of the pseudo I order model;  $q_e$  = the amounts of  $\text{Cr}^{6+}$  biosorbed at equilibrium;  $R^2$  = correlation coefficient of the model;  $k_2$  = rate constant of second-order adsorption;  $\alpha$  = initial adsorption rate of Elovich model;  $\beta$  = desorption constant of Elovich model;  $k_{diff}$  = intraparticle diffusion rate constant;  $C_e$  = parameter related to the boundary layer thickness.

The fit of the experimental data to Elovich model indicates that the rate of  $\text{Cr}^{6+}$  biosorption decreases exponentially as the amount of  $\text{Cr}^{6+}$  biosorbed increase. The graphical representations of the models, as well as the values of the correlation coefficients, highlighted that the pseudo II order model can also describe the  $\text{Cr}^{6+}$  biosorption, with  $R^2$  greater than 0.845. However, from the comparison of the calculated uptake capacity values with the experimental ones, it can be observed that a major difference exists between them, indicating that this model is not suitable to describe the kinetics of  $\text{Cr}^{6+}$  biosorption by *B. megaterium* and *Rhodotorula* sp.

### 3.7. Biosorption Isotherms

Linear analysis of isotherm data into isotherm models are commonly used, but several researchers have shown that transforming adsorption isotherms into their linearized forms leads to maximization of errors between experimental data and the respective isotherm [59–62]. So, in this study, the nonlinear forms of Langmuir, Freundlich, Redlich-Peterson, Javanovic, Hill and Dual Mode models were considered for modelling of biosorption isotherms. The isotherm model that best describes the biosorption of chromium ions was established based on correlation coefficients ( $R^2$ ) calculated in Origin Pro 8 software. In Figures 8 and 9, the graphical representation of the nonlinear forms of the Langmuir, Freundlich, Redlich-Peterson, Javanovic, Hill and Dual Mode models applied to the isotherm data of  $\text{Cr}^{6+}$  biosorption by *B. megaterium* and *Rhodotorula* sp. are shown. The values of the characteristic parameters of each model are included in Table 4. For the  $\text{Cr}^{6+}$  biosorption by the inactive biomass of *B. megaterium* and *Rhodotorula* sp. was found that that Freundlich isotherm is the model that best fits with the biosorption data, with the correlation coefficient values of 0.9432 and 0.9382, respectively. According to the description of this model, multi-layer biosorption occurred and was performed on heterogeneous surfaces with uniformly distributed energy. During the  $\text{Cr}^{6+}$  biosorption the stronger binding centers were occupied first, then the others. This model also indicates that the biosorption process of  $\text{Cr}^{6+}$  ions is favorable under the given experimental conditions, since the value of the parameter  $n$  is between 1 and 10 ( $n = 4.817$  for *B. megaterium* and  $n = 3.734$  for *Rhodotorula* sp.).

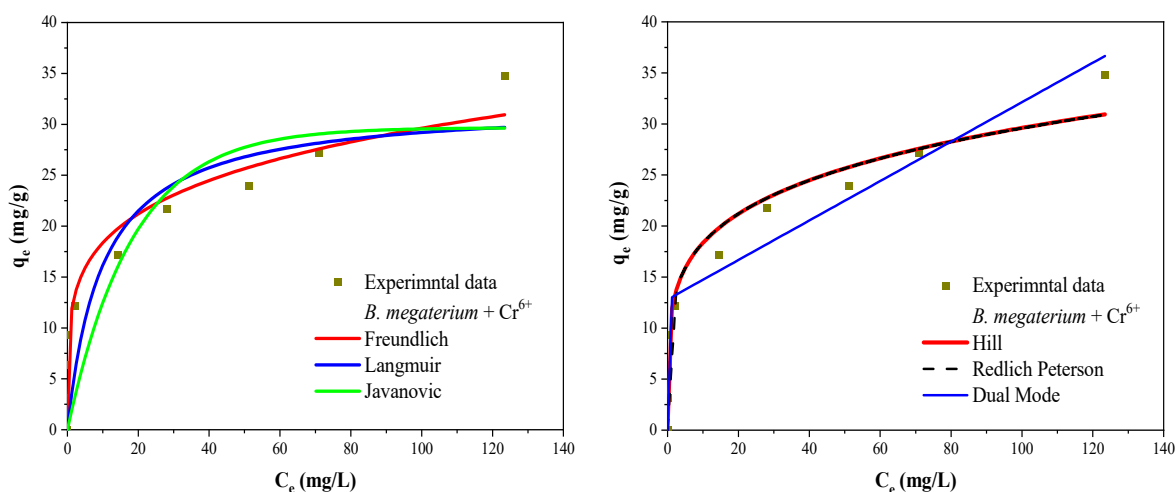


**Figure 8.** Graphical representation of adsorption isotherms applied to experimental data of  $\text{Cr}^{6+}$  biosorption by *Bacillus megaterium* inactive biomass.

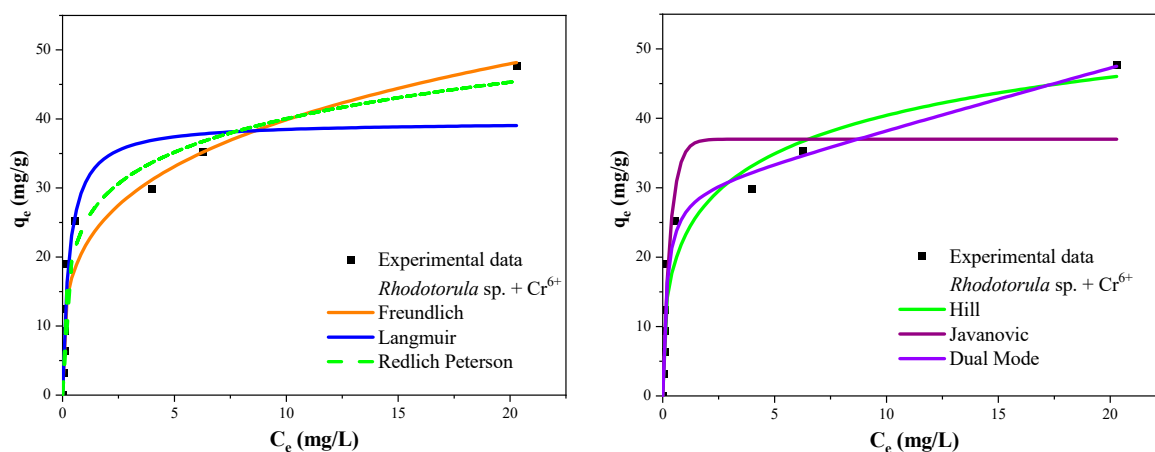


**Figure 9.** Graphical representation of adsorption isotherms applied to experimental data of  $\text{Cr}^{6+}$  biosorption by *Rhodotorula* sp. inactive biomass.

**Table 4.** Values of isotherm parameters applied to experimental data from the chromium ion biosorption.

Isotherm Model	Isotherm Parameters	<i>B. megaterium</i>		<i>Rhodotorula</i> sp.	
		Parameter Value	SE	Parameter Value	SE
Langmuir	$q_m$ (mg/g)	32.072	5.292	39.597	3.392
	$b$ (L/mg)	0.101	0.078	3.426	1.158
	$R_L$	0.281–0.024	-	0.011–0.0007	-
	$R^2$	0.7788	-	0.8829	-
Freundlich	$k$ (mg/g)	11.382	1.436	21.516	1.851
	$n$	4.817	0.739	3.734	0.511
	$R^2$	0.9432	-	0.9382	-
Redlich-Peterson	$A_R$ (L/g)	$9.383 \times 10^7$	$4.282 \times 10^6$	260.71	200.22
	$B_R$ (mg/mL)	$8.223 \times 10^6$	$3.772 \times 10^5$	9.47	8.988
	$m_R$	0.793	0.041	0.831	0.083
	$R^2$	0.9351	-	0.9167	-
Jovanovic	$q_m$ (mg/g)	29.671	4.129	36.993	3.363
	$K_J$ (L/mg)	0.054	0.028	2.942	0.929
	$R^2$	0.7357	-	0.8522	-
Hill	$q_m$ (mg/g)	$3.169 \times 10^6$	$3.02 \times 10^5$	79.681	71.36
	$K_D$	278,679.31	$2.66 \times 10^4$	2.451	3.445
	$n_H$	0.207	0.111	0.402	0.194
	$R^2$	0.9351	-	0.9015	-
Dual Mode	$q_m$ (mg/g)	12.815	1.591	29.899	3.970
	$K_d$ (L/g)	0.193	0.026	0.880	0.306
	$b$ (L/mg)	284.31	215.75	5.713	2.035
	$R^2$	0.9386	-	0.9077	-
$q_{max}$ experimental (mg/g)		34.808	0.019	47.70	0.115

SE = Standard Error;  $R^2$  = correlation coefficient of the model;  $q_m$  = the maximum amount of metal ions adsorbed;  $b$  = Langmuir constant;  $R_L$  = separation factor;  $k$  = Freundlich constants;  $1/n$  = Freundlich constants related to the adsorption intensity;  $A_R$  = Redlich-Peterson isotherm constant;  $B_R$  = model constant;  $m_R$  = model exponent;  $K_J$  = Jovanovic constant;  $n_H$  = Hill cooperativity coefficient of the binding interaction;  $K_D$  = Hill constant;  $K_d$  = the partitioning constant of Dual Mode model;  $b$  = the adsorption constant.

### 3.8. FTIR and SEM-EDS Analysis of the Biosorbent

Through FTIR analysis, it was possible to identify the different functional groups in the cell wall structure and to identify the chemical bonds that had a significant contribution to the biosorption of hexavalent chromium. In various studies, it has been highlighted that the aldehydes, alkyl chains, amides, amines, alcohols/phenols, carboxylic compounds, esters, organic halogens, phosphate, sulfoxide and aliphatic organic chains could be responsible for hexavalent chromium biosorption [63–67]. The FTIR spectra of chromium-unloaded and chromium-loaded biomass of *B. megaterium* and *Rhodotorula* sp. are shown in Figure 10. The IR spectra of the native biomass and  $\text{Cr}^{6+}$  loaded biomass showed that the peak intensities were slightly different, finding that some peaks were slightly shifted and some FTIR peaks appeared after chromium biosorption. The band assignments of the FTIR peaks that changed after chromium biosorption are presented in Table 5. Each absorption band in the IR spectra indicates the presence of a particular functional group on the biosorbent surface. Stretching vibrations of hydroxyl groups, P=O symmetric and asymmetric stretching of phosphate groups, hydroxyl groups from polysaccharides, C–O stretching of alcoholic groups, deformation vibration of C=O carboxylic acids, C–N stretching in amide II group and N–H bending were identified on the surface of the biosorbents, and which changed their absorption bands after  $\text{Cr}^{6+}$  contact [66,67]. The FTIR analysis revealed that the changes observed may be due to the interaction between chromium and functional groups (i.e., amino, hydroxyl, and carboxyl groups) found on the biosorbent surface. For example, the wavenumber of the OH stretching vibration on *B. megaterium* decreased from

3476.05 to 3402.84  $\text{cm}^{-1}$  and on *Rhodotorula* sp. increased from 3391.28 to 3410.55  $\text{cm}^{-1}$ . According to Petrović et al. [68] these changes may be due the possible complexation process.

**Table 5.** IR absorption peaks of the functional groups identified on the biosorbents surface that have been modified after  $\text{Cr}^{6+}$  biosorption.

Peak		Types of Vibration	Ref.
Native Biomass	$\text{Cr}^{6+}$ Loaded Biomass		
<i>Bacillus megaterium</i>			
-	836.67	S=O stretching	[65,67,69–72]
1064.01	1060.15	P=O symmetric stretching of phosphate groups, –OH group of polysaccharides; C–O stretching of alcoholic groups, of ethers	
1233.54	1229.69	P=O asymmetric stretching of phosphate groups, carbonyl stretch C=O of carboxylic acid	
1545.65	1541.79	C–N stretching in amide II group and N–H bending	
1649.68	1653.53	C=O and C–N stretching in amide I group	
3476.05	3402.84	Stretching vibrations of hydroxyl groups	
<i>Rhodotorula</i> sp.			
1033.18	1029.33	P=O symmetric stretching of phosphate groups, –OH group of polysaccharides; C–O stretching of alcoholic groups, of ethers	[65,67,69–72]
1152.63	1156.48	P=O asymmetric stretching of phosphate groups, carbonyl stretch C=O of carboxylic acid	
1403.08	1399.23	–COO <sup>−</sup> symmetric stretching of carboxyl groups	
1457.02	1460.87	–CH <sub>2</sub> bending, symmetric C=O	
3391.28	3410.55	Stretching vibrations of hydroxyl groups	

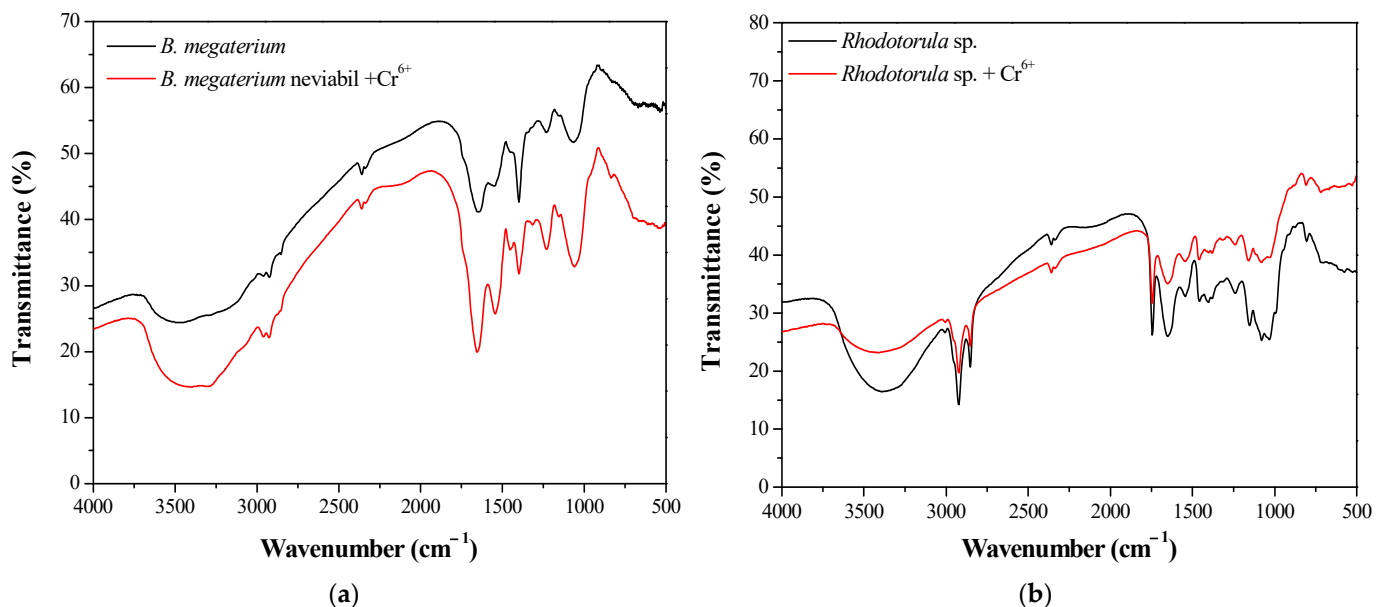


**Figure 10.** IR spectra recorded for (a) *Bacillus megaterium* and (b) *Rhodotorula* sp. before and after  $\text{Cr}^{6+}$  biosorption.

Textural characteristics of *B. megaterium* and *Rhodotorula* sp. as well as possible changes of the biosorbent surface after  $\text{Cr}^{6+}$  biosorption were observed by SEM analysis. Biosorbents were scanned and images obtained at  $\times 3000$  magnification are shown in Figures 11 and 12. SEM images showed that the microorganisms used for chromium biosorption change their structural aspects after ion contact. The cells of microorganisms had well-defined shapes, but after chromium biosorption, the cells appear to coalesce and are deformed, their shape being irregular compared to the regular rod or rounded shape of the native

cells. These changes highlighted that  $\text{Cr}^{6+}$  biosorption caused cell wall destruction due to the involvement of functional groups on the cell surface in ion removal.

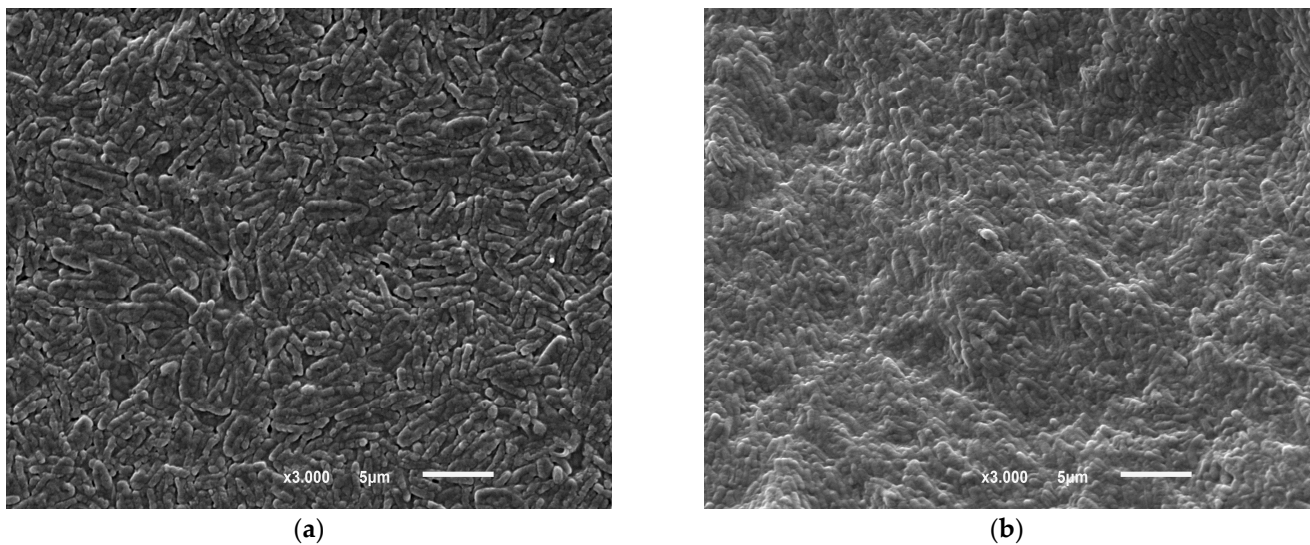


**Figure 11.** SEM analysis of *Bacillus megaterium* surface (a) before and (b) after  $\text{Cr}^{6+}$  biosorption.

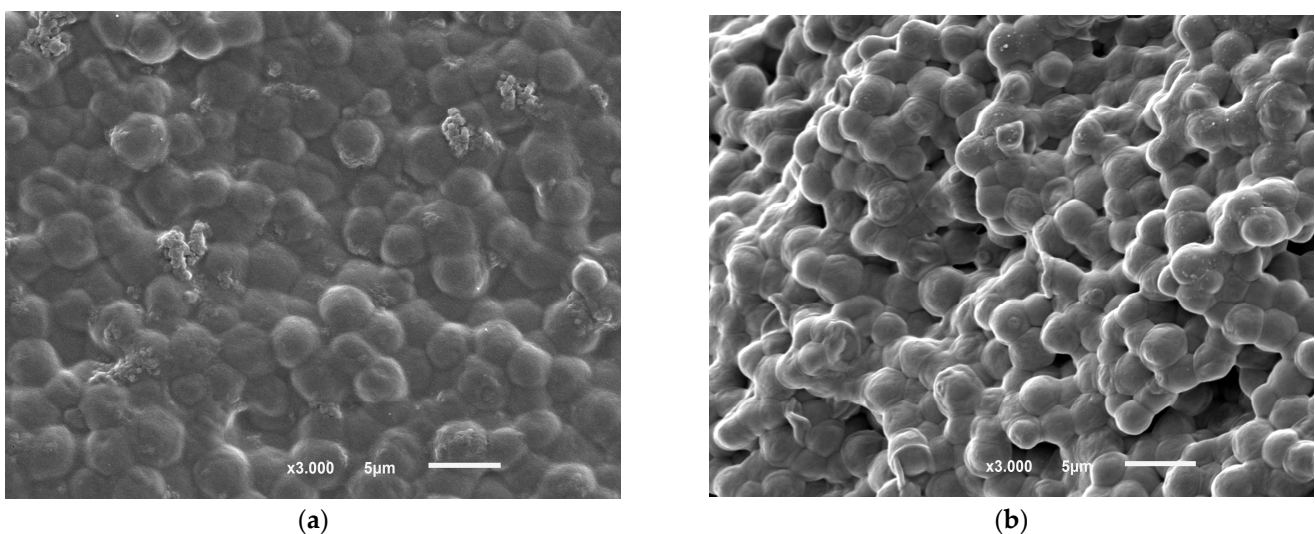


**Figure 12.** SEM analysis of *Rhodotorula* sp. surface (a) before and (b) after  $\text{Cr}^{6+}$  biosorption.

EDX analysis of the biosorbents was performed at the same time as SEM analysis at 5 kV voltage and provided information about the concentration and distribution of elements in the biosorbent biomass. The results of these analyses, which are illustrated in Figure 13, highlighted that at the end of the process no chromium was found in the composition of the biosorbents.

By linking the SEM-EDX analysis with the FTIR spectra, process efficiency and with the information provided by the Freundlich isotherm and the Elovich model, it can be asserted that extracellular reduction is the main mechanism involved in  $\text{Cr}^{6+}$  biosorption by the selected biosorbents.

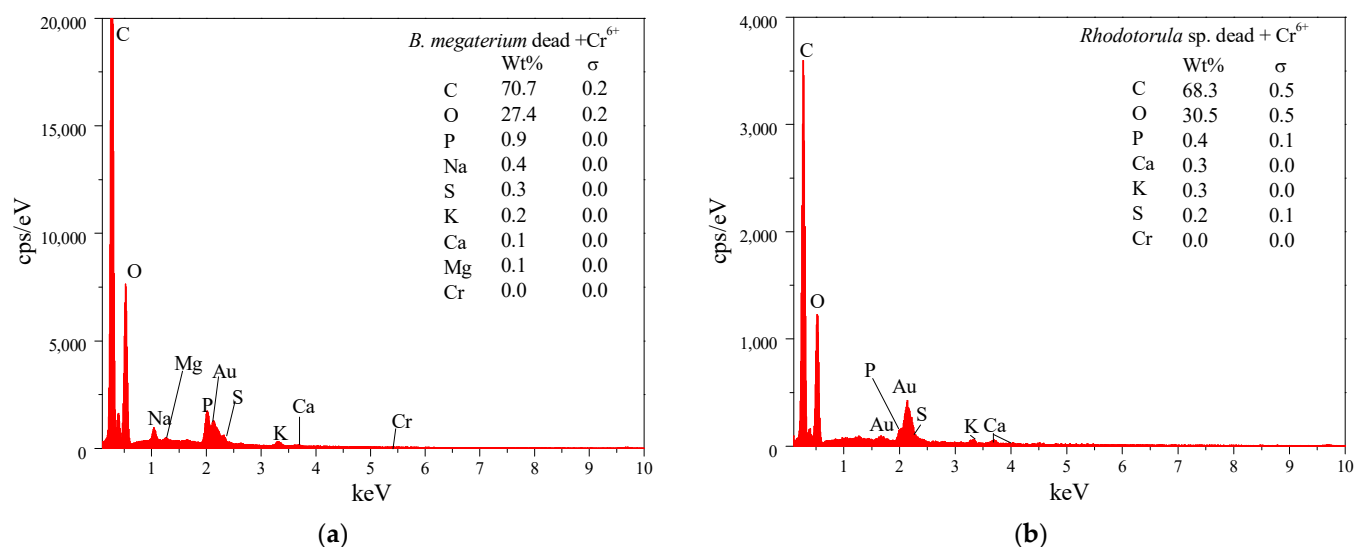


**Figure 13.** Elemental composition of biosorbents: (a) *Bacillus megaterium* and (b) *Rhodotorula* sp. after Cr<sup>6+</sup> ions biosorption.

#### 4. Conclusions

Chromium is one of the most dangerous pollutants found in industrial effluents in two stable forms (trivalent and hexavalent chromium). Although both forms of chromium have harmful effects, the hexavalent form is highly toxic to all living organisms even in low (trace) concentrations. Thus, the removal of hexavalent chromium from industrial wastewater has become extremely important in water pollution control and in attempting to minimize the associated risks to human health.

The results of this study proved one more time that microorganisms are able to remove metal ions from aqueous solutions. This work highlights the potential of *B. megaterium* and *Rhodotorula* sp. for the removal of Cr<sup>6+</sup> from aqueous solutions. The experimental results showed that Cr<sup>6+</sup> biosorption follows the Elovich model, which suggests that the rate of Cr<sup>6+</sup> biosorption decreases exponentially as the amount of Cr<sup>6+</sup> biosorbed increases. The Freundlich model best describes the Cr<sup>6+</sup> biosorption equilibrium data for *B. megaterium* and *Rhodotorula* sp. and indicates that multilayer biosorption mainly controls this process and is done on heterogeneous surfaces with uniformly distributed energy. During the Cr<sup>6+</sup> biosorption, the stronger binding centers were occupied first, then the others. This model also indicates that the biosorption process of Cr<sup>6+</sup> ions is favorable under the given experimental conditions, since the value of the parameter  $n$  is between 1 and 10 ( $n = 4.817$  for *B. megaterium* and  $n = 3.734$  for *Rhodotorula* sp.). The uptake capacities of 34.80 mg/g and 47.70 mg/g were achieved by *Bacillus megaterium* and *Rhodotorula* sp. at pH 1, biosorbent dosage of 8 g/L, 25 °C, after a contact time of 48 h and an initial Cr<sup>6+</sup> concentration in solution of 402.52 mg/L.

By linking the SEM-EDX results with the FTIR spectra, the removal efficiencies of Cr<sup>6+</sup> and total chromium and with the information provided by the Freundlich isotherm and the Elovich model, it can be asserted that extracellular reduction is the main mechanism involved in Cr<sup>6+</sup> biosorption by the selected biosorbents.

**Author Contributions:** Conceptualization, M.R. and M.G.; methodology, M.R., B.S. and T.T.; formal analysis, M.R.; investigation, M.R.; data curation, M.R.; writing—original draft preparation, M.R.; writing—review and editing, M.R. and B.S.; visualization, B.S., T.T. and M.G.; supervision, M.G. and T.T. All authors have read and agreed to the published version of the manuscript.

**Funding:** This research received no external funding.

**Data Availability Statement:** Not applicable.

**Conflicts of Interest:** The authors declare no conflict of interest.



## References

1. European Environment Agency. The European Pollutant Release and Transfer Register (E-PRTR), Member States Reporting under Article 7 of Regulation (EC) No 166/2006—European Environment Agency. Available online: <https://www.eea.europa.eu/data-and-maps/data/member-states-reporting-art-7-under-the-european-pollutant-release-and-transfer-register-e-prtr-regulation-10> (accessed on 11 December 2020).
2. Namieśnik, J.; Rabajczyk, A. The Speciation and Physico-Chemical Forms of Metals in Surface Waters and Sediments. *Chem. Speciat. Bioavailab.* **2010**, *22*, 1–24. [\[CrossRef\]](#)
3. Ozturk, B.C. Mapping of Selected Trace Metals and Associated Risk in Coastal Sediments along the Northwest Anatolia Coasts of Turkey. *Environ. Eng. Manag. J.* **2021**, *20*, 1999–2012. [\[CrossRef\]](#)
4. Abubeah, R.; Altaher, H.; Khalil, T. Removal of Hexavalent Chromium Using Two Innovative Adsorbents. *Environ. Eng. Manag. J.* **2018**, *17*, 1621–1634. [\[CrossRef\]](#)
5. Diaconu, M.; Rosca, M.; Cozma, P.; Minut, M.; Smaranda, C.; Hlihor, R.-M.; Gavrilesco, M. Toxicity and Microbial Bioremediation of Chromium Contaminated Effluents. In Proceedings of the 2020 International Conference on E-Health and Bioengineering (EHB), Iasi, Romania, 29–30 October 2020; pp. 1–4.
6. Langård, S.; Costa, M. Chromium. In *Handbook on the Toxicology of Metals*; Elsevier: Amsterdam, The Netherlands, 2015; pp. 717–742. ISBN 978-0-444-59453-2.
7. WHO Chromium. *Air Quality Guidelines*; WHO Regional Office for Europe: Copenhagen, Denmark, 2000.
8. Daulton, T.L.; Little, B.J. Determination of Chromium Valence over the Range Cr(0)–Cr(VI) by Electron Energy Loss Spectroscopy. *Ultramicroscopy* **2006**, *106*, 561–573. [\[CrossRef\]](#)
9. Saha, R.; Nandi, R.; Saha, B. Sources and Toxicity of Hexavalent Chromium. *J. Coord. Chem.* **2011**, *64*, 1782–1806. [\[CrossRef\]](#)
10. Tchounwou, P.B.; Yedjou, C.G.; Patlolla, A.K.; Sutton, D.J. Heavy Metal Toxicity and the Environment. In *Molecular, Clinical and Environmental Toxicology: Volume 3: Environmental Toxicology*; Experientia Supplementum; Luch, A., Ed.; Springer: Basel, Switzerland, 2012; pp. 133–164, ISBN 978-3-7643-8340-4.
11. Daniel, R.; Anjaneyulu, Y.; Krupadam, R.J. Cr (VI) Removal from Electroplating Industrial Effluents: A Greener and Cheaper Method. *Zaštita Mater.* **2009**, *50*, 13–18.
12. Sibi, G. Biosorption of Chromium from Electroplating and Galvanizing Industrial Effluents under Extreme Conditions Using *Chlorella Vulgaris*. *Green Energy Environ.* **2016**, *1*, 172–177. [\[CrossRef\]](#)
13. Verma, S.K.; Khandegar, V.; Saroha, A.K. Removal of Chromium from Electroplating Industry Effluent Using Electrocoagulation. *J. Hazard. Toxic Radioact. Waste* **2013**, *17*, 146–152. [\[CrossRef\]](#)
14. Sharma, D.; Chaudhari, P.K.; Prajapati, A.K. Removal of Chromium (VI) and Lead from Electroplating Effluent Using Electrocoagulation. *Sep. Sci. Technol.* **2020**, *55*, 321–331. [\[CrossRef\]](#)
15. Abdulla, H.M.; Kamal, E.M.; Mohamed, A.H.; El-Bassuony, A.D. Chromium Removal from Tannery Wastewater Using Chemical and Biological Techniques Aiming Zero Discharge of Pollution. In Proceeding of Fifth Scientific Environmental Conference, Houston, TX, USA, 12–16 July 2010; pp. 171–183.
16. Liu, C.-C.; Wang, M.-K.; Chiou, C.-S.; Li, Y.-S.; Lin, Y.-A.; Huang, S.-S. Chromium Removal and Sorption Mechanism from Aqueous Solutions by Wine Processing Waste Sludge. *Ind. Eng. Chem. Res.* **2006**, *45*, 8891–8899. [\[CrossRef\]](#)
17. Rosca, M.; Hlihor, R.-M.; Gavrilesco, M. Bioremediation of Persistent Toxic Substances: From Conventional to New Approaches in Using Microorganisms and Plants. In *Microbial Technology for the Welfare of Society*; Microorganisms for Sustainability; Arora, P.K., Ed.; Springer: Singapore, 2019; Volume 17, pp. 289–312, ISBN 9789811388439.
18. Gavrilesco, M. Removal of Heavy Metals from the Environment by Biosorption. *Eng. Life Sci.* **2004**, *4*, 219–232. [\[CrossRef\]](#)
19. Hammoudani, Y.E.; Dimane, F.; Ouarghi, H.E. Removal Efficiency of Heavy Metals by a Biological Wastewater Treatment Plant and Their Potential Risks to Human Health. *Environ. Eng. Manag. J.* **2021**, *8*, 995–1002. [\[CrossRef\]](#)
20. Bulgariu, L.; Gavrilesco, M. Bioremediation of Heavy Metals by Microalgae. In *Handbook of Marine Microalgae*; Elsevier: Amsterdam, The Netherlands, 2015; pp. 457–469, ISBN 978-0-12-800776-1.
21. Hlihor, R.; Petronela, C.; Gavrilesco, M. Removal of Heavy Metals from the Environment by Phytoremediation and Microbial Remediation. In *Sustainable Solutions for Environmental Pollution*; El-Gendy, N.S., Ed.; Wiley: Hoboken, NJ, USA, 2022; pp. 95–146, ISBN 978-1-119-82751-1.
22. Filote, C.; Roşca, M.; Hlihor, R.M.; Cozma, P.; Simion, I.M.; Apostol, M.; Gavrilesco, M. Sustainable Application of Biosorption and Bioaccumulation of Persistent Pollutants in Wastewater Treatment: Current Practice. *Processes* **2021**, *9*, 39. [\[CrossRef\]](#)
23. Chwastowski, J.; Staroń, P. Influence of *Saccharomyces Cerevisiae* Yeast Cells Immobilized on *Cocos Nucifera* Fibers for the Adsorption of Pb(II) Ions. *Colloids Surf. A Physicochem. Eng. Asp.* **2022**, *632*, 127735. [\[CrossRef\]](#)
24. Uysal, O.G.; Demir, A.; Gören, N. Investigation of Cobalt(II) Adsorption from Aqueous. *Environ. Eng. Manag. J.* **2022**, *21*, 637–650. [\[CrossRef\]](#)
25. Abdi, O.; Kazemi, M. A Review Study of Biosorption of Heavy Metals and Comparison between Different Biosorbents. *J. Mater. Environ. Sci.* **2015**, *6*, 1386–1399.
26. Bulgariu, L.; Bulgariu, D.; Rusu, C. Marine Algae Biomass for Removal of Heavy Metal Ions. In *Hb25\_Springer Handbook of Marine Biotechnology*; Kim, S.-K., Ed.; Springer: Berlin/Heidelberg, Germany, 2015; pp. 611–648, ISBN 978-3-642-53970-1.
27. Shamim, S. Biosorption of Heavy Metals. In *Biosorption*; Derco, J., Vrana, B., Eds.; InTech: London, UK, 2018; ISBN 978-1-78923-472-5.

28. Filote, C.; Roșca, M.; Simion, I.M.; Hlihor, R.M. Continuous Systems Bioremediation of Wastewaters Loaded with Heavy Metals Using Microorganisms. *Processes* **2022**, *10*, 1758. [CrossRef]
29. Hlihor, R.M.; Diaconu, M.; Fertu, D.; Chelaru, C.; Sandu, I.; Tavares, T. Bioremediation of Cr(VI) Polluted Wastewaters by Sorption on Heat Inactivated *Saccharomyces Cerevisiae* Biomass. *Int. J. Environ. Res.* **2013**, *7*, 581–594. [CrossRef]
30. Hlihor, R.M.; Diaconu, M.; Leon, F.; Curteanu, S.; Tavares, T.; Gavrilescu, M. Experimental Analysis and Mathematical Prediction of Cd(II) Removal by Biosorption Using Support Vector Machines and Genetic Algorithms. *New Biotechnol.* **2015**, *32*, 358–368. [CrossRef]
31. Ganguly, A.; Guha, A.K.; Ray, L. Adsorption Behaviour of Cadmium by *Bacillus Cereus* M<sup>16</sup>: Some Physical and Biochemical Studies. *Chem. Speciat. Bioavailab.* **2011**, *23*, 175–182. [CrossRef]
32. Li, Z.; Yuan, H. Responses of *Rhodotorula* sp. Y11 to Cadmium. *Biometals* **2008**, *21*, 613–621. [CrossRef] [PubMed]
33. Upadhyay, N.; Vishwakarma, K.; Singh, J.; Mishra, M.; Kumar, V.; Rani, R.; Mishra, R.K.; Chauhan, D.K.; Tripathi, D.K.; Sharma, S. Tolerance and Reduction of Chromium(VI) by *Bacillus* sp. MNU16 Isolated from Contaminated Coal Mining Soil. *Front. Plant Sci.* **2017**, *8*, 778. [CrossRef] [PubMed]
34. Roșca, M.; Hlihor, R.-M.; Cozma, P.; Drăgoi, E.N.; Diaconu, M.; Silva, B.; Tavares, T.; Gavrilescu, M. Comparison of *Rhodotorula* sp. and *Bacillus megaterium* in the Removal of Cadmium Ions from Liquid Effluents. *Green Process. Synth.* **2018**, *7*, 74–88. [CrossRef]
35. US EPA. SW-846 Test Method 7196A: Chromium, Hexavalent (Colorimetric). Available online: <https://www.epa.gov/hw-sw846/sw-846-test-method-7196a-chromium-hexavalent-colorimetric> (accessed on 15 August 2022).
36. Kajjumba, G.W.; Emik, S.; Öngen, A.; Kurtulus Özcan, H.; Aydın, S. Modelling of Adsorption Kinetic Processes—Errors, Theory and Application. In *Advanced Sorption Process Applications*; Edebali, S., Ed.; IntechOpen: London, UK, 2019; ISBN 978-1-78984-818-2.
37. Netzahuatl-Muñoz, A.R.; del Carmen Cristiani-Urbina, M.; Cristiani-Urbina, E. Chromium Biosorption from Cr(VI) Aqueous Solutions by *Cupressus lusitanica* Bark: Kinetics, Equilibrium and Thermodynamic Studies. *PLoS ONE* **2015**, *10*, e0137086. [CrossRef]
38. An, B. Cu(II) and As(V) Adsorption Kinetic Characteristic of the Multifunctional Amino Groups in Chitosan. *Processes* **2020**, *8*, 1194. [CrossRef]
39. Rangabhashiyam, S.; Anu, N.; Giri Nandagopal, M.S.; Selvaraju, N. Relevance of Isotherm Models in Biosorption of Pollutants by Agricultural Byproducts. *J. Environ. Chem. Eng.* **2014**, *2*, 398–414. [CrossRef]
40. Saadi, R.; Saadi, Z.; Fazaali, R.; Fard, N.E. Monolayer and Multilayer Adsorption Isotherm Models for Sorption from Aqueous Media. *Korean J. Chem. Eng.* **2015**, *32*, 787–799. [CrossRef]
41. Ayawei, N.; Ebelegi, A.N.; Wankasi, D. Modelling and Interpretation of Adsorption Isotherms. *J. Chem.* **2017**, *2017*, 3039817. [CrossRef]
42. Torkia, Y.B.; Bouaziz, N.; Al-Muhtaseb, S.A.; Lamine, A.B. Adsorption Energy and Pore-Size Distributions of Activated Carbons Calculated Using Hill's Model. *Adsorpt. Sci. Technol.* **2014**, *32*, 571–590. [CrossRef]
43. Misra, D.N. Jovanovich Adsorption Isotherm for Heterogeneous Surfaces. *J. Colloid Interface Sci.* **1973**, *43*, 85–88. [CrossRef]
44. Vieth, W.R.; Sladek, K.J. A Model for Diffusion in a Glassy Polymer. *J. Colloid Sci.* **1965**, *20*, 1014–1033. [CrossRef]
45. Gonen, Y.; Rytwo, G. Using the Dual-Mode Model to Describe Adsorption of Organic Pollutants onto an Organoclay. *J. Colloid Interface Sci.* **2006**, *299*, 95–101. [CrossRef]
46. Aranda-García, E.; Cristiani-Urbina, E. Hexavalent Chromium Removal and Total Chromium Biosorption from Aqueous Solution by *Quercus Crassipes* Acorn Shell in a Continuous Up-Flow Fixed-Bed Column: Influencing Parameters, Kinetics, and Mechanism. *PLoS ONE* **2020**, *15*, e0227953. [CrossRef] [PubMed]
47. Jobby, R.; Jha, P.; Gupta, A.; Gupte, A.; Desai, N. Biotransformation of Chromium by Root Nodule Bacteria *Sinorhizobium* sp. SAR1. *PLoS ONE* **2019**, *14*, e0219387. [CrossRef]
48. Hlihor, R.M.; Figueiredo, H.; Tavares, T.; Gavrilescu, M. Biosorption Potential of Dead and Living *Arthrobacter Viscosus* Biomass in the Removal of Cr(VI): Batch and Column Studies. *Process Saf. Environ. Prot.* **2017**, *108*, 44–56. [CrossRef]
49. da Rocha Ferreira, G.L.; Vendruscolo, F.; Antoniosi Filho, N.R. Biosorption of Hexavalent Chromium by *Pleurotus Ostreatus*. *Heliyon* **2019**, *5*, e01450. [CrossRef] [PubMed]
50. Fernández-López, J.A.; Angosto, J.M.; Avilés, M.D. Biosorption of Hexavalent Chromium from Aqueous Medium with *Opuntia* Biomass. *Sci. World J.* **2014**, *2014*, 670249. [CrossRef]
51. Ojiagu, D.K.; Odibo, C.F.J.; Ojiagu, C.; Agu, K.C.; Okafor, A.C. Biosorption of Hexavalent Chromium by *Pseudomonas Aeruginosa* Strain ANSC: Equilibria Isothermic, Kinetic and Thermodynamic Studies. *Bioeng. Biosci.* **2018**, *6*, 1–10. [CrossRef]
52. Srinath, T.; Verma, T.; Ramteke, P.W.; Garg, S.K. Chromium (VI) Biosorption and Bioaccumulation by Chromate Resistant Bacteria. *Chemosphere* **2002**, *48*, 427–435. [CrossRef]
53. Al-Ghouti, M.A.; Al-Absi, R.S. Mechanistic Understanding of the Adsorption and Thermodynamic Aspects of Cationic Methylene Blue Dye onto Cellulosic Olive Stones Biomass from Wastewater. *Sci. Rep.* **2020**, *10*, 15928. [CrossRef]
54. Volesky, B. Biosorption Process Simulation Tools. *Hydrometallurgy* **2003**, *71*, 179–190. [CrossRef]
55. Tang, X.; Huang, Y.; Li, Y.; Wang, L.; Pei, X.; Zhou, D.; He, P.; Hughes, S.S. Study on Detoxification and Removal Mechanisms of Hexavalent Chromium by Microorganisms. *Ecotoxicol. Environ. Saf.* **2021**, *208*, 111699. [CrossRef]
56. Pagnanelli, F. Equilibrium, Kinetic and Dynamic Modelling of Biosorption Processes. In *Microbial Biosorption of Metals*; Kotrba, P., Mackova, M., Macek, T., Eds.; Springer: Dordrecht, The Netherlands, 2011; pp. 59–120. ISBN 978-94-007-0442-8.
57. Rosca, M.; Hlihor, R.M.; Cozma, P.; Simion, I.M.; Filote, C.; Grecu, C.; Stoleru, V.; Gavrilescu, M. Scaling-Up Strategies of Heavy Metals Microbial Bioremediation. In Proceedings of the 2021 International Conference on e-Health and Bioengineering (EHB), Iasi, Romania, 18–19 November 2021; pp. 1–4.

58. Temel, F.A.; Avci, E.; Turan, N.G. Investigation of Copper(II), Zinc(II) and Lead(II) Removal onto Expanded Perlite by Adsorption from the Wastes of Metal Casting Industry: Statistical Modeling and Optimization. *Environ. Eng. Manag. J.* **2022**, *21*, 757–767. [[CrossRef](#)]
59. Shahmohammadi-Kalalagh, S.; Babazadeh, H.; Nazemi, A. Comparison of Linear and Nonlinear Forms of Isotherm Models for Zn(II) and Cu(II) Sorption on a Kaolinite. *Arab J Geosci* **2015**, *8*, 397–402. [[CrossRef](#)]
60. Tsai, S.-C.; Juang, K.-W. Comparison of Linear and Nonlinear Forms of Isotherm Models for Strontium Sorption on a Sodium Bentonite. *J. Radioanal. Nucl. Chem.* **2000**, *243*, 741–746. [[CrossRef](#)]
61. Yaneva, Z.L.; Koumanova, B.K.; Georgieva, N.V. Linear and Nonlinear Regression Methods for Equilibrium Modelling of *p*-Nitrophenol Biosorption by *Rhizopus Oryzae*: Comparison of Error Analysis Criteria. *J. Chem.* **2013**, *2013*, 517631. [[CrossRef](#)]
62. Rosca, M.; Diaconu, M.; Hlihor, R.-M.; Cozma, P.; Gavrilescu, M. Prediction of Equilibrium Sorption Isotherm for Cadmium Biosorption by Microorganisms: Comparison of Linear and Nonlinear Methods. In Proceedings of the 2020 International Conference on e-Health and Bioengineering (EHB), Iasi, Romania, 29–30 October 2020; pp. 1–4.
63. Ayele, A.; Godeto, Y.G. Bioremediation of Chromium by Microorganisms and Its Mechanisms Related to Functional Groups. *J. Chem.* **2021**, *2021*, 7694157. [[CrossRef](#)]
64. Rahman, Z.; Thomas, L. Chemical-Assisted Microbially Mediated Chromium (Cr) (VI) Reduction Under the Influence of Various Electron Donors, Redox Mediators, and Other Additives: An Outlook on Enhanced Cr(VI) Removal. *Front. Microbiol.* **2021**, *11*, 619766. [[CrossRef](#)] [[PubMed](#)]
65. Hossan, S.; Hossain, S.; Islam, M.R.; Kabir, M.H.; Ali, S.; Islam, M.S.; Imran, K.M.; Moniruzzaman, M.; Mou, T.J.; Parvez, A.K.; et al. Bioremediation of Hexavalent Chromium by Chromium Resistant Bacteria Reduces Phytotoxicity. *Int. J. Environ. Res. Public Health* **2020**, *17*, 6013. [[CrossRef](#)]
66. Petrović, M.; Šoštarić, T.; Stojanović, M.; Petrović, J.; Mihajlović, M.; Ćosović, A.; Stanković, S. Mechanism of Adsorption of Cu<sup>2+</sup> and Zn<sup>2+</sup> on the Corn Silk (*Zea mays* L.). *Ecol. Eng.* **2017**, *99*, 83–90. [[CrossRef](#)]
67. Simić, M.; Petrović, J.; Šoštarić, T.; Ercegović, M.; Milojković, J.; Lopičić, Z.; Kojić, M. A Mechanism Assessment and Differences of Cadmium Adsorption on Raw and Alkali-Modified Agricultural Waste. *Processes* **2022**, *10*, 1957. [[CrossRef](#)]
68. Petrović, M.; Šoštarić, T.; Stojanović, M.; Milojković, J.; Mihajlović, M.; Stanojević, M.; Stanković, S. Removal of Pb<sup>2+</sup> Ions by Raw Corn Silk (*Zea mays* L.) as a Novel Biosorbent. *J. Taiwan Inst. Chem. Eng.* **2016**, *58*, 407–416. [[CrossRef](#)]
69. Pradhan, D.; Sukla, L.B.; Mishra, B.B.; Devi, N. Biosorption for Removal of Hexavalent Chromium Using Microalgae *Scenedesmus* sp. *J. Clean. Prod.* **2019**, *209*, 617–629. [[CrossRef](#)]
70. Talari, A.C.S.; Martinez, M.A.G.; Movasaghi, Z.; Rehman, S.; Rehman, I.U. Advances in Fourier Transform Infrared (FTIR) Spectroscopy of Biological Tissues. *Appl. Spectrosc. Rev.* **2017**, *52*, 456–506. [[CrossRef](#)]
71. Duygu, D.Y.; Udoh, A.U.; Ozer, T.B.; Akbulut, A.; Erkaya, I.A.; Yildiz, K.; Guler, D. Fourier Transform Infrared (FTIR) Spectroscopy for Identification of *Chlorella vulgaris* Beijerinck 1890 and *Scenedesmus obliquus* (Turpin) Kützing 1833. *Afr. J. Biotechnol.* **2012**, *11*, 3817–3824. [[CrossRef](#)]
72. Shan, B.; Hao, R.; Xu, H.; Zhang, J.; Li, J.; Li, Y.; Ye, Y. Hexavalent Chromium Reduction and Bioremediation Potential of *Fusarium Proliferatum* S4 Isolated from Chromium-Contaminated Soil. *Environ. Sci. Pollut. Res.* **2022**, *29*, 78292–78302. [[CrossRef](#)]

**Disclaimer/Publisher's Note:** The statements, opinions and data contained in all publications are solely those of the individual author(s) and contributor(s) and not of MDPI and/or the editor(s). MDPI and/or the editor(s) disclaim responsibility for any injury to people or property resulting from any ideas, methods, instructions or products referred to in the content.